Stem Cell Reports, Volume *17*

Supplemental Information

Functional redundancy among Polycomb complexes in maintaining the pluripotent state of embryonic stem cells

Yaru Zhu, Lixia Dong, Congcong Wang, Kunying Hao, Jingnan Wang, Linchun Zhao, Lijun Xu, Yin Xia, Qing Jiang, and Jinzhong Qin

Supplementary Materials for

Functional redundancy among Polycomb complexes in maintaining the pluripotent state of embryonic stem cells

Yaru Zhu[1†], Lixia Dong[1†], Congcong Wang[1†], Kunying Hao[1†], Jingnan Wang[1], Linchun Zhao[1], Lijun Xu[1], Yin Xia[2], Qing Jiang[3], Jinzhong Qin[1,4*]

*Correspondence author. Email: qinjz@nju.edu.cn

The PDF file includes:

Figs. S1 to S6

Tables S6 to S8

Other Supplementary Material for this manuscript includes the following:

Tables S1 to S5

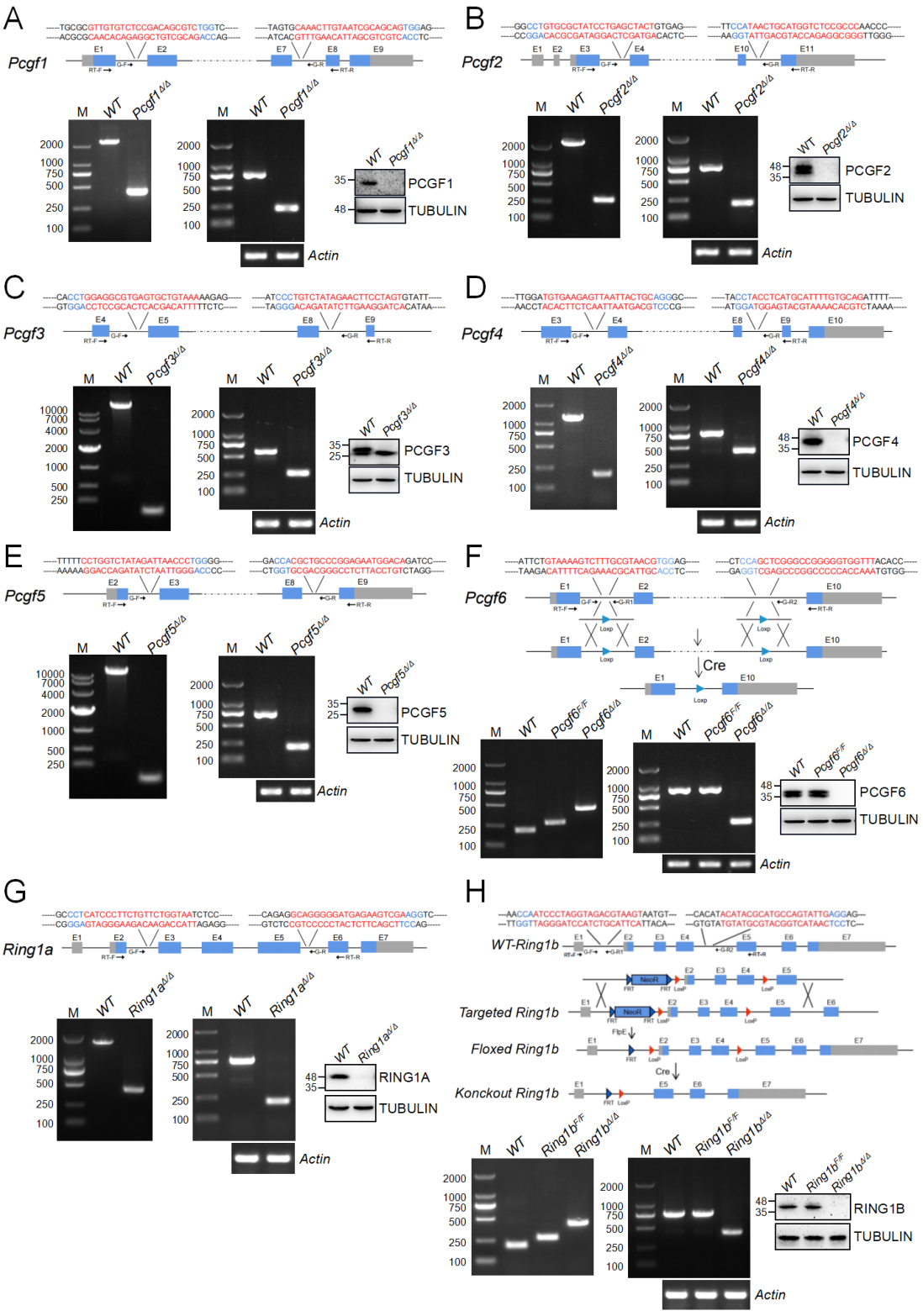

Figure S1. Generation of knockout ESC lines of *Pcgf* family, *Ring1a* and *Ring1b*. Related to Figures 1 to 3. (**A** to **H**) Top, schematic representation of CRISPR/Cas9 mediated knockout approaches to generate ESCs deficient in *Pcgf* family, *Ring1a* and *Ring1b*. PAM sequences are in blue following the sgRNA sequence highlighted in red. The locations of genomic PCR primers (G-F, Forward; G-R, Reverse) and RT-PCR primers (RT-F, Forward; RT-R, Reverse) are shown. Bottom, genotyping of ESCs with

indicated gene deletions using primers located upstream and downstream of the deleted region (left); RT-PCR analysis for residual mRNA revealed a shorter band in the mutants (middle). The absence of the protein is confirmed by using western blot (right).TUBULIN acted as a loading control.

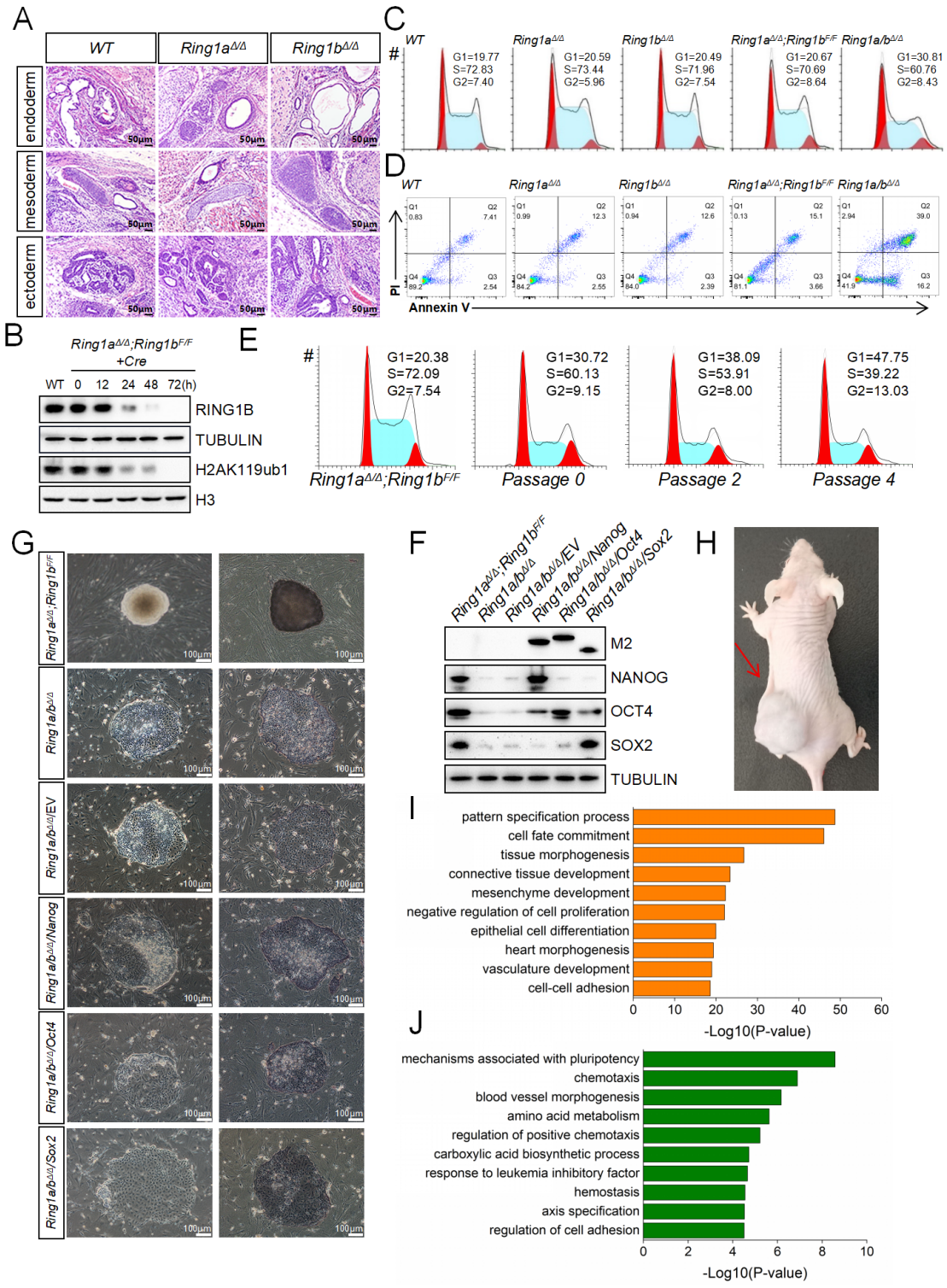

Figure S2. *Ring1a/b* play redundant and crucial roles in ESC self-renewal and maintenance. Related to Figure 3. (**A**) Representative images showing H&E staining of histological sections derived from teratomas generated from ESCs of the indicated genotypes. Shown is a representative of three injected mice. Scale bars, 50 μm. (**B**) Western blot showing RING1B and H2AK119ub1 levels in *Ring1a*$^{\Delta/\Delta}$*;Ring1b*$^{F/F}$ ESCs-transfected Cre recombinase for different time points. (**C**) Detection of changes in cell-cycle profile changes in cell-cycle profile determined by PI staining and FACS analysis. (**D**) Determination of apoptosis by flow cytometry of Annexin V/PI staining in ESCs of indicated genotypes. The percentages of Annexin V–positive (apoptotic) cells are within the two right quadrants. (**E**) Detection of changes in cell-cycle profile in *Ring1a*$^{\Delta/\Delta}$*;Ring1b*$^{F/F}$ following lenti-Cre infection determined by PI staining and FACS analysis. (**F**) Western blot demonstrating the levels of pluripotency factors in ESCs of indicated genotypes. The expression levels of the indicated FLAG-tagged proteins were detected with anti-Flag M2 antibody. Tubulin acted as a loading control. (**G**) Phase-contrast images of ESC colonies of indicated genotypes on MEF feeders (left). Representative images of AP staining of ESC colonies of indicated genotypes (right). (**H**) Representative images of mice bearing teratomas 28d after the injection of *Ring1a*$^{\Delta/\Delta}$*;Ring1b*$^{F/F}$ (left side, indicated by a red arrow) or *Ring1a/b*$^{\Delta/\Delta}$ ESCs (right side). Four mice were injected per condition. (**I and J**) Gene ontology analysis of overlapping genes up-regulated (**I**) and down-regulated (**J**) in *Ring1a*$^{\Delta/\Delta}$, *Ring1b*$^{\Delta/\Delta}$, and *Ring1a/b*$^{\Delta/\Delta}$ ESCs.

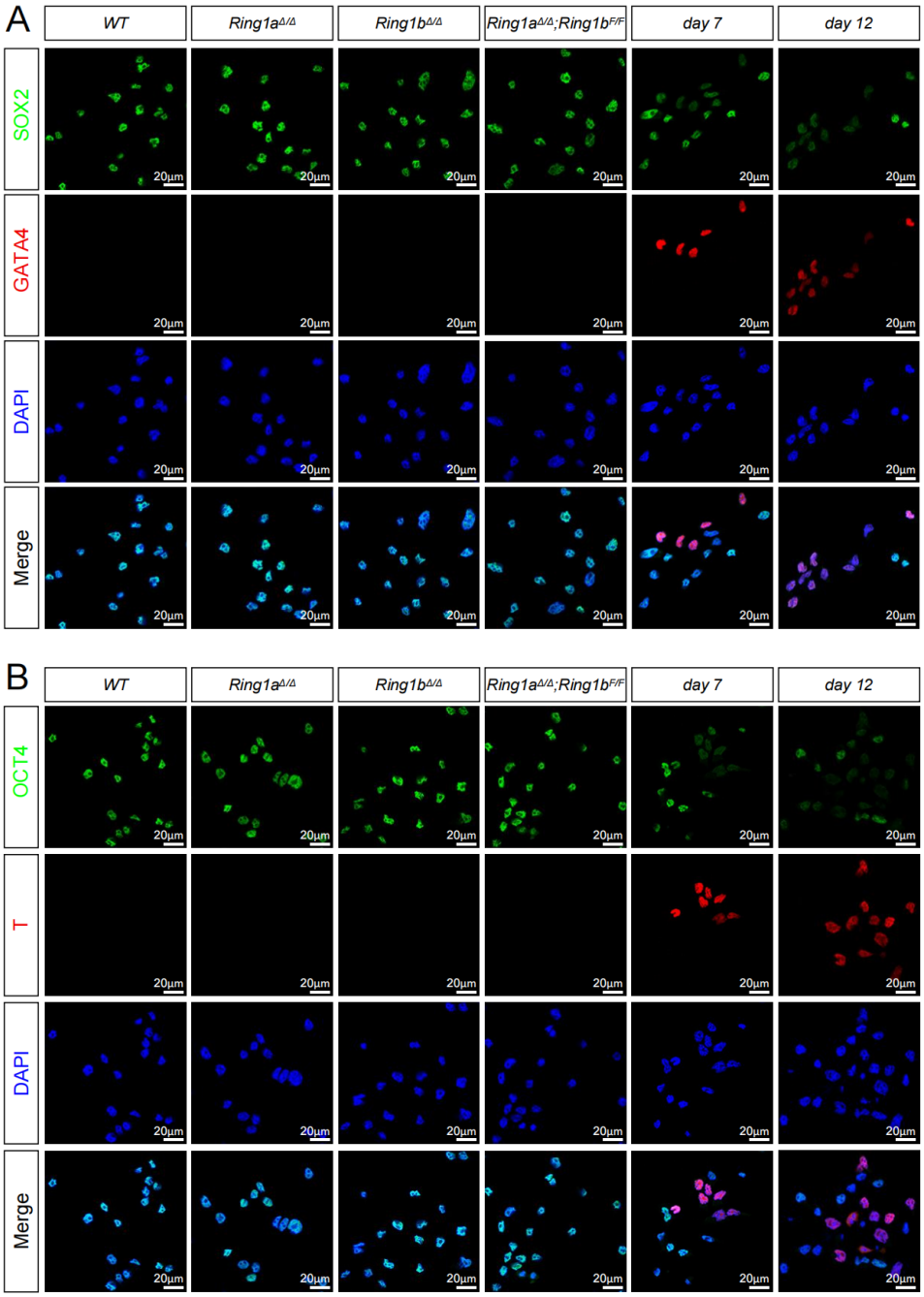

Figure S3. Combined *Ring1a/b* depletion triggers activation of lineage-specific genes and results in exit from ESC pluripotency. Related to Figure 3. IF analysis for SOX2, OCT4 (green), GATA4, T (red) or DAPI (blue) in *Ring1a*$^{\Delta/\Delta}$, *Ring1b*$^{\Delta/\Delta}$, and *Ring1a*$^{\Delta/\Delta}$*;Ring1b*$^{F/F}$ ESCs following lenti-Cre infection. Pictures were taken at 63x magnification using confocal microscopy. Merge, merged images.

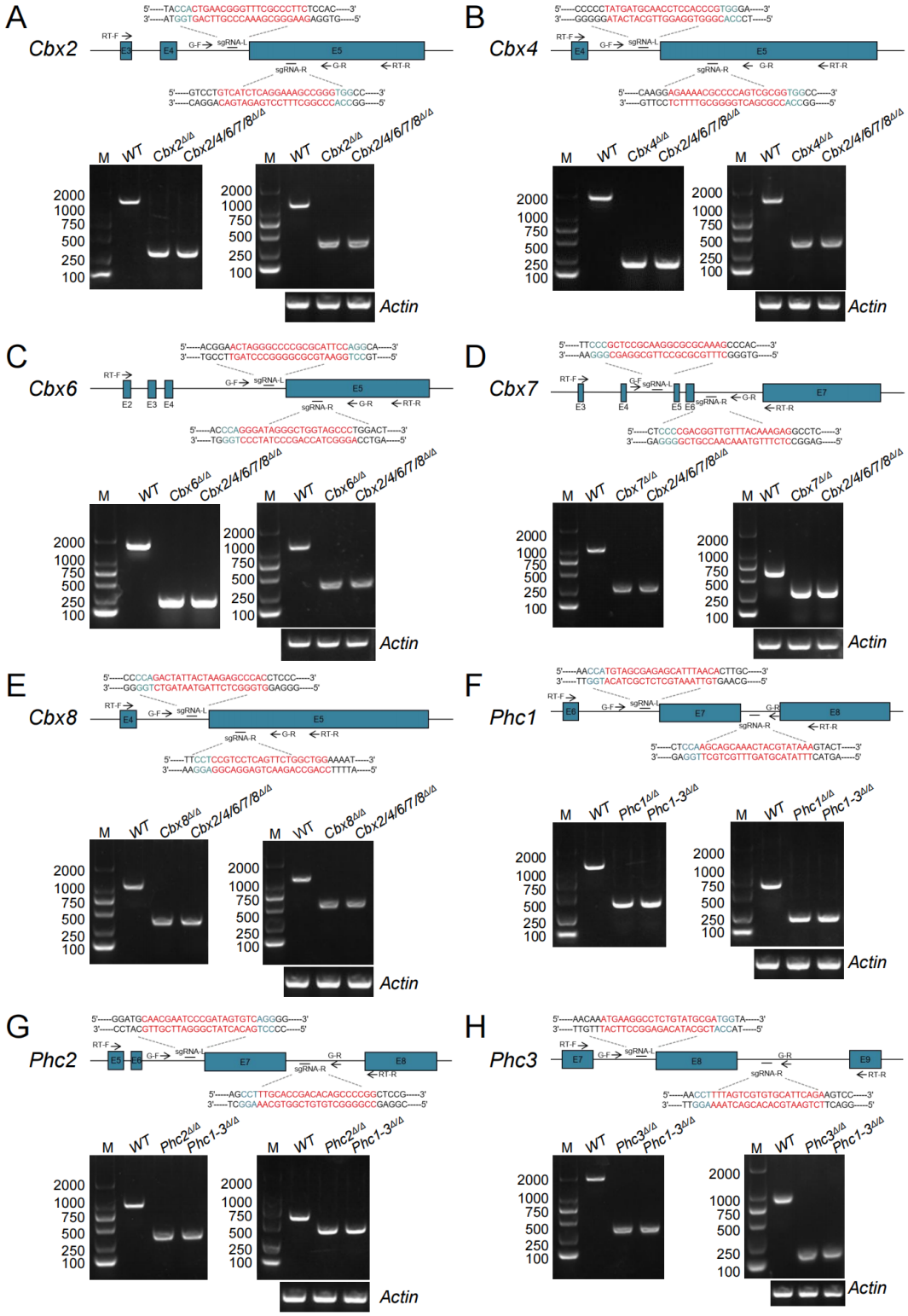

Figure S4. Generation of single and combined knockout ESC lines of *Cbx2/4/6/7/8* and *Phc1-3*. Related to Figure 4. (**A** to **H**) Top, schematic representation of CRISPR/Cas9 mediated knockout approaches to generate ESCs deficient in *Cbx2/4/6/7/8* and *Phc1-3*. PAM sequences are in blue following the sgRNA sequence highlighted in red. The locations of genomic PCR primers (G-F, Forward; G-R, Reverse) and RT-PCR primers (RT-F, Forward; RT-R, Reverse) are shown. Bottom, genotyping of ESCs

with indicated gene deletions using primers located upstream and downstream of the deleted region (left); RT-PCR analysis for residual mRNA revealed a shorter band in the mutants (right). *β-Actin* acted as a loading control.

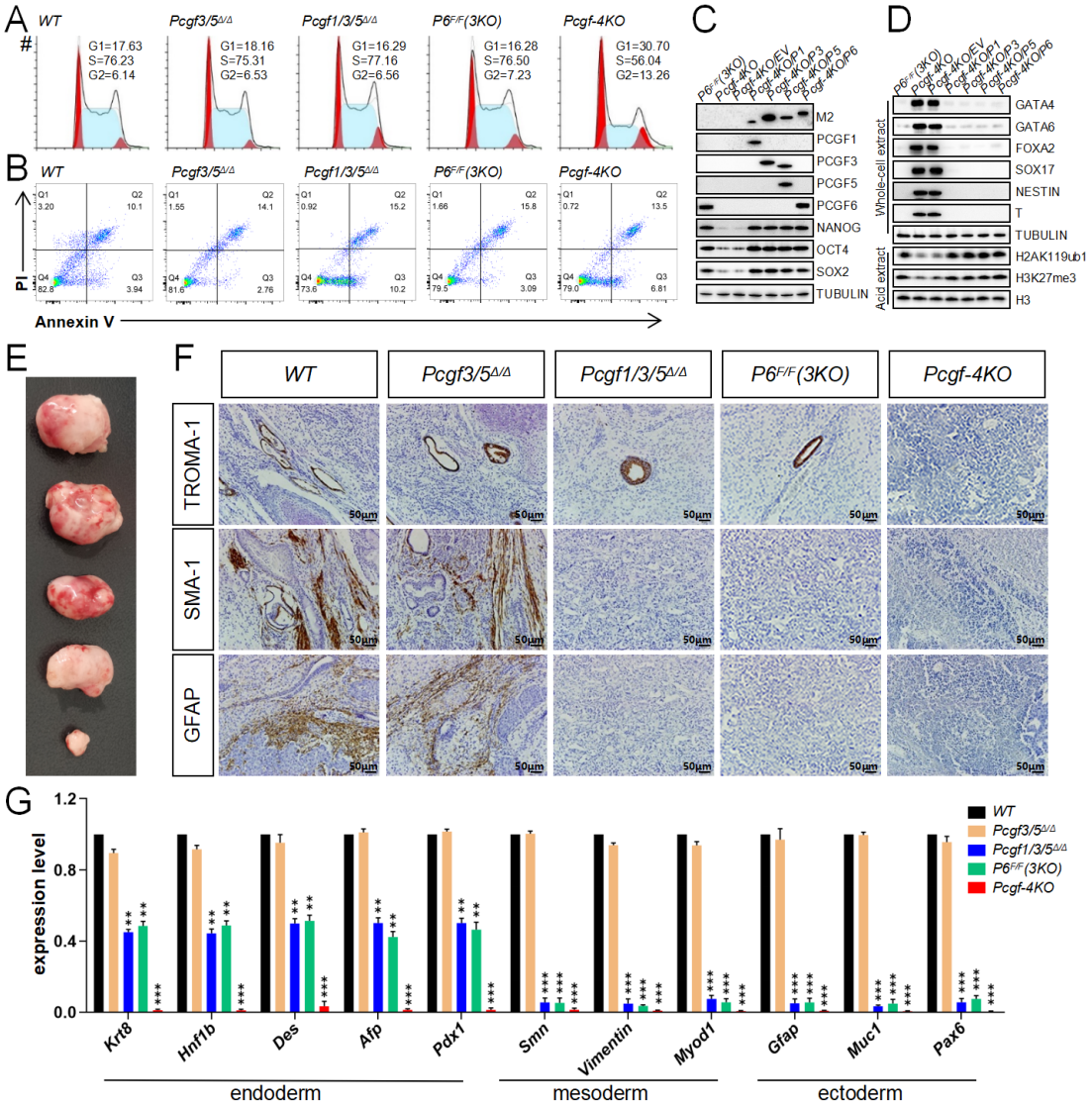

Figure S5. Disruption of ncPRC1 leads to profound differentiation defects in ESCs. Related to Figure 5. (**A**) Representative cell cycle profiles determined by PI-staining and FACS analysis. (**B**) Flow cytometric quantification of apoptosis with Annexin-V and PI. The percentages of Annexin V–positive (apoptotic) cells are within the two right quadrants. (**C** and **D**) Western blot demonstrating changes in the levels of selected PcG proteins, pluripotency factors, (**D**) germ layer markers and histone modifications, in ESCs of indicated genotypes. The expression levels of the indicated FLAG-tagged proteins were detected with anti-Flag M2 antibody. TUBULIN and H3 were used as loading controls. (**E**) Teratoma formation in immunodeficiency mice by *WT*, *Pcgf3/5*$^{\Delta/\Delta}$, *Pcgf1/3/5*$^{\Delta/\Delta}$, *Pcgf1/3/5*$^{\Delta/\Delta}$*;Pcgf6*$^{F/F}$ and *Pcgf1/3/5/6*$^{\Delta/\Delta}$ ESCs (from top to bottom) 28d after injection. (n=3 animals for each condition). (**F**) Immunohistochemical analysis of teratomas corresponding to the indicated genotypes using markers for endoderm (TROMA1) (top), mesoderm (smooth muscle actin 1 [SMA1]) (middle) and ectoderm (GFAP) (bottom). The scale bar is 50μm. (**G**) RT-qPCR analysis of the three germ layer markers in indicated

teratomas. Each value was normalized to its corresponding *actin* value and the expression level in WT ESCs was arbitrarily set to 1. Data are shown as the means ± SD for triplicate analysis. *p < 0.05, **p < 0.01, ***p < 0.001 (Student's t test) compared with the control.

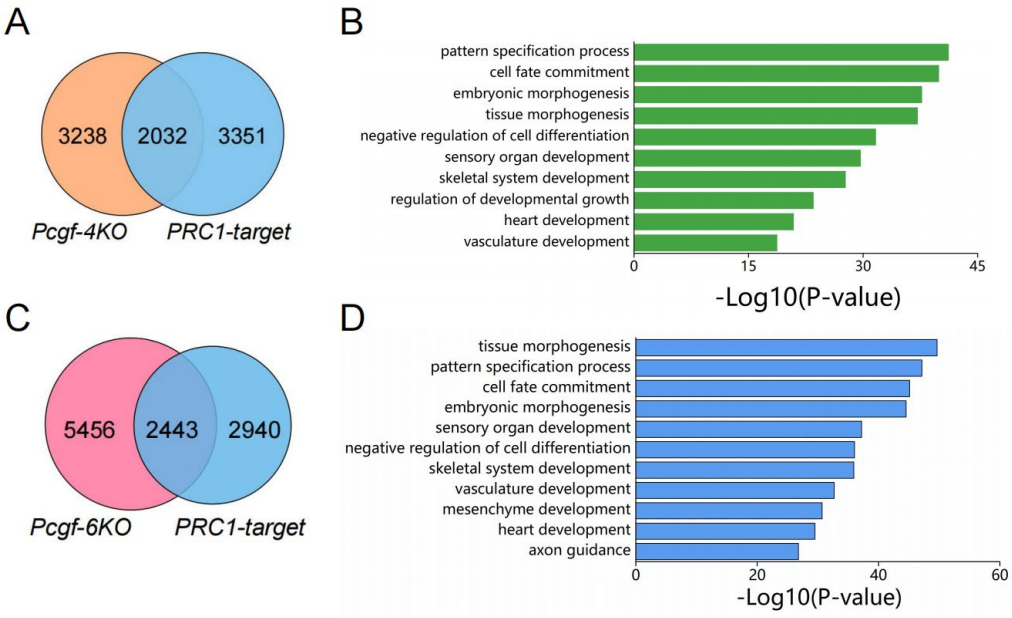

Figure S6. *Pcgf* shares target genes with PRC1, Related to Figure 7. (**A and C**) Venn diagram showing the overlap between genes differentially expressed after *Pcgf* deletion and those occupied by PRC1. (**B and D**) GO analysis for biological processes associated with the overlapping genes.

Table S1. Genes that are differentially expressed in *Ring1a*$^{\Delta/\Delta}$ vs. control ESCs.
Table S2. Genes that are differentially expressed in *Ring1b*$^{\Delta/\Delta}$ vs. control ESCs.
Table S3. Genes that are differentially expressed in *Ring1a/b*$^{\Delta/\Delta}$ vs. control ESCs.
Table S4. Genes that are differentially expressed in *Pcgf1/3/5/6*$^{\Delta/\Delta}$ vs. control ESCs.
Table S5. Genes that are differentially expressed in *Pcgf1/2/3/4/5/6*$^{\Delta/\Delta}$ vs. control ESCs.

Table S6: Cell lines used in this study

Cell Lines	Source（Original Validation）
Ezh1$^{\Delta/\Delta}$	(Huang et al., 2021) （Figure S5）
Ezh2$^{\Delta/\Delta}$	(Huang et al., 2021)（Figure S5）
Suz12$^{\Delta/\Delta}$	(Huang et al., 2021)（Figure S5）
Eed$^{\Delta/\Delta}$	(Huang et al., 2021)（Figure S5）
Jarid2$^{\Delta/\Delta}$	(Huang et al., 2021)（Figure S6）
Aebp2$^{\Delta/\Delta}$	(Huang et al., 2021)（Figure S6）
Phf1$^{\Delta/\Delta}$	(Huang et al., 2021)（Figure S6）
Mtf2$^{\Delta/\Delta}$	(Huang et al., 2021)（Figure S6）
Phf19$^{\Delta/\Delta}$	(Huang et al., 2021)（Figure S6）
Pcgf1$^{\Delta/\Delta}$	this study
Pcgf2$^{\Delta/\Delta}$	this study
Pcgf3$^{\Delta/\Delta}$	this study
Pcgf4$^{\Delta/\Delta}$	this study
Pcgf5$^{\Delta/\Delta}$	this study
Pcgf6$^{\Delta/\Delta}$	this study
Bcor$^{\Delta/\Delta}$	(Qin et al., 2021)（Figure S1）
Bcorl1$^{\Delta/\Delta}$	(Qin et al., 2021)（Figure S1）
Skp1$^{\Delta/\Delta}$	(Qin et al., 2021)（Figure S1）
Cbx2$^{\Delta/\Delta}$	This study
Cbx4$^{\Delta/\Delta}$	This study
Cbx6$^{\Delta/\Delta}$	This study
Cbx7$^{\Delta/\Delta}$	This study
Cbx8$^{\Delta/\Delta}$	This study
Hp1γ$^{\Delta/\Delta}$	(Qin et al., 2021)（Figure S1）
Hdac1$^{\Delta/\Delta}$	(Qin et al., 2021)（Figure S1）
Hdac2$^{\Delta/\Delta}$	(Qin et al., 2021)（Figure S1）
E2f6$^{\Delta/\Delta}$	(Qin et al., 2021)（Figure S1）
G9a$^{\Delta/\Delta}$	(Qin et al., 2021)（Figure S1）
Glp$^{\Delta/\Delta}$	(Qin et al., 2021)（Figure S1）
Rybp$^{\Delta/\Delta}$	(Zhao et al., 2018)（Figure S3）
Yaf2$^{\Delta/\Delta}$	(Zhao et al., 2018)（Figure S1）
Ring1a$^{\Delta/\Delta}$	This study
Ring1b$^{\Delta/\Delta}$	This study

Usp7$^{\Delta/\Delta}$	(Qin et al., 2021)（Figure S1）
Kdm2b$^{\Delta/\Delta}$	(Qin et al., 2021)（Figure S1）
Scmh1$^{\Delta/\Delta}$	(Qin et al., 2021)（Figure S1）
Scml2$^{\Delta/\Delta}$	(Qin et al., 2021)（Figure S1）
Phc1$^{\Delta/\Delta}$	This study
Phc2$^{\Delta/\Delta}$	This study
Phc3$^{\Delta/\Delta}$	This study
Ck2α1$^{\Delta/\Delta}$	(Qin et al., 2021)（Figure S1）
Ck2α2$^{\Delta/\Delta}$	(Qin et al., 2021)（Figure S1）
Ck2b$^{\Delta/\Delta}$	(Qin et al., 2021)（Figure S1）
Auts2$^{\Delta/\Delta}$	(Qin et al., 2021)（Figure S1）
Fbrs$^{\Delta/\Delta}$	(Qin et al., 2021)（Figure S1）
Fbrsl1$^{\Delta/\Delta}$	(Qin et al., 2021)（Figure S1）
Mga$^{\Delta/\Delta}$	(Qin et al., 2021)（Figure S1）
Max$^{\Delta/\Delta}$	(Qin et al., 2021)（Figure S1）
Dp-1$^{\Delta/\Delta}$	(Qin et al., 2021)（Figure S1）
Wdr5$^{\Delta/\Delta}$	(Qin et al., 2021) (Figure S1）
L3mbtl2$^{\Delta/\Delta}$	(Huang et al., 2018)（Figure S2）
Cbx2/4/6/7/8$^{\Delta/\Delta}$	this study
Rybp/Yaf2$^{\Delta/\Delta}$	(Zhao et al., 2018)（Figure S1 and S3）
Phc1/2/3$^{\Delta/\Delta}$	this study
Ring1a$^{\Delta/\Delta}$*;Ring1b*$^{F/F}$	this study
Ring1a/b$^{\Delta/\Delta}$	this study
Pcgf3/5$^{\Delta/\Delta}$	this study
Pcgf2/4$^{\Delta/\Delta}$	this study
Pcgf1/3/5$^{\Delta/\Delta}$	this study
Pcgf1/3/5$^{\Delta/\Delta}$*;Pcgf6*$^{F/F}$	this study
Pcgf1/3/5/6$^{\Delta/\Delta}$	this study
Pcgf1/2/3/4/5$^{\Delta/\Delta}$	this study
Pcgf1/2/3/4/5$^{\Delta/\Delta}$*;Pcgf6*$^{F/F}$	this study
Pcgf1/2/3/4/5/6$^{\Delta/\Delta}$	this study

Table S7: Summary of the primers used in this study

Gene Name	Forward Primer	Reverse Primer	Application
Cbx2	CTAATCTCCCTCCCGGTTCC	GGGGAGGGAGCTGTATCAGT	Genomic-PCR
Cbx4	CACGAGCCCTTCCCTAAACAT	TCCTATAGGGAAGGGGACGTG	Genomic-PCR
Cbx6	CACACACGATGACTTAGGGGT	ATGGCGAGATAGCACCGAGA	Genomic-PCR
Cbx7	CCAAGGGCAATGAGAAGCTC	CCACGGATCAGCCTCTGAAA	Genomic-PCR
Cbx8	AGGACTTAGCTGCACCAGAA	CTCCACACACCCTCCAAAATCC	Genomic-PCR
Phc1	TTTGGTTCTGTGGCTTTGGT	ACAAGGCAAGCACACACAAA	Genomic-PCR
Phc2	AGCTAGGTTATGAGTCCGGC	GTCACCCTCCTTTACCTCCC	Genomic-PCR

Phc3	ACACTTACTTGGGAAGCTTTCT	CTTTTAACTGAGAACTAAT	Genomic-PCR
Cbx2	GAACATTTTGGACCCGAGGC	ACCTCACAGTAGTTGGCCAG	RT-PCR
Cbx4	TGAAATGGAGAGGCTGGTCC	TCCTATAGGGAAGGGGACGTG	RT-PCR
Cbx6	AGGAAAGGGAACGTGAGCTG	CCAAACACTGCACACAGAGC	RT-PCR
Cbx7	GGAGCACATCTTGGACCCT	GTTGTCCTGATCCTGTCCCC	RT-PCR
Cbx8	AAAGGGAACGGGAGATGGAG	TCCCCTACCAAACCACAGTC	RT-PCR
Phc1	AGTCTCCTGGAGTTCATGCA	TGTTGGAACTGTTGCTGGTG	RT-PCR
Phc2	AGCCAAGCACAGATGTACCT	CTTGTGGACATGCGTGGTAG	RT-PCR
Phc3	CACTCGGACATCAAGCATCC	CATCCTTGCACACTCATCGG	RT-PCR
Afp	TATGGACTCTCAGGCTGCTG	GCCCTGTTTTCTTCATGTGC	RT-PCR
Sox7	GACCCTGGCTTCCTCCTC	GAGTACTCACCCCTGTCCTC	RT-PCR
Gata4	TCTCTTTCCCGGGGACTACT	GGTAGGGGCTGGAGTAGGAG	RT-PCR
Hnf1b	CTTGGAGGAGTTACTGCCGT	CGTGGCCATTGGTGAGAGTA	RT-PCR
Gata6	CTCTGCACGCTTTCCCTACT	GTAGGTCGGGTGATGGTGAT	RT-PCR
Foxa2	GACATACCGACGCAGCTACA	GGCACCTTGAGAAAGCAGTC	RT-PCR
Otx1	CGGAAGCTATGGTCAGGGAT	TGAAGATTGGCTCAGTGGGT	RT-PCR
Meis	GTTCACCACCTAAACCACGG	CGTTGACAGCAGATCCCATG	RT-PCR
Lhx5	ACCTCAACTGCTTCACCTGT	AGTAGTCGTCCTTGCACACA	RT-PCR
Nestin	CAACCTTGCCGAAGAGCTG	GCATTCTTCTCCGCCTCGA	RT-PCR
Krt18	GACCATGCAAGACCTGAACG	GCCCCTTCTTCTCCAGATGT	RT-PCR
Bmp4	TCTTTACCGGCTCCAGTCTG	AACTCCTCACAGTGTTGGCT	RT-PCR
Eomes	AAGCGTCCAAGAAGTTTCCG	GTCCGCGTCACTGAGCAT	RT-PCR
Bmp6	CTCTTCTTCGGGCTTCCTCT	CTGAGGCTGCTGGAGACC	RT-PCR
Msx2	CGCTCATGTCCGACAAGAAG	ATTTTCCGACTTGACCGAGG	RT-PCR
T	TCCCGGTGCTGAAGGTAAAT	CCCACTCCCCGTTCACATAT	RT-PCR
Hand1	GAGCGGCCTTACTTCCAGA	GGTCCTGAGCCTTTTCGTTT	RT-PCR
Tead4	TGCAGAGGGTGTATGGAGC	ATCTTGCCTTCCTCCGTCAG	RT-PCR
zeb1	AGCTGACTGTGAAGGTGGC	CGTTGTCTTGCCAGCAGTT	RT-PCR
Actin	AGCCATGTACGTAGCCATCC	CTCTCAGCTGTGGTGGTGAA	RT-PCR
Vim	GCTTCAAGACTCGGTGGACT	TTTTGTTCTGCTGCTCGAGG	RT-PCR
Ema	GCATTCGGGCTCCTTTCTTC	TCTGAGTTGCTGCTGTGGA	RT-PCR
Des	CCAGGCCTACTCGTCCAG	GCGGGATGTCATTGAACTCG	RT-PCR
Pdx1	ACACAGCTCTACAAGGACCC	ACTTCCCTGCTCCAGTGATC	RT-PCR
Myod1	TCCGGGACATAGACTTGACAG	TGCTCCTCCGGTTTCAGG	RT-PCR
Pax6	TCTGCAGGTATCCAACGGTT	GCAAAGATGGAAGGGCACTC	RT-PCR
Krt8	GTGAACCAGAGCCTGTTGAG	CATCTTGTTCTGCTGCTCCA	RT-PCR
Smn	CCGGCCAGAGTGATGATTCT	GCAGGTTTTCTTCTGGCTGT	RT-PCR
Gfap	ACGCTTCTCCTTGTCTCGAA	CGGACCTTCTCGATGTAGCT	RT-PCR
Pcgf1	CTGTGTGAACCCAAACGAAGG	GTCATGTGATCTGGGAGAACCT	Genomic-PCR
Pcgf2	CCACCCTGGCTCATAGAGAT	AGGAAGAGGCCAGCAGTAAG	Genomic-PCR
Pcgf3	GCTCTTGCCCCTTAGTGACT	TCTAAGCACAGTGACAGCCA	Genomic-PCR
Pcgf4	CTGTTACATGAAAGGCCTACCT	TCTGTCGTCAAGATCTAACCCA	Genomic-PCR
Pcgf5	GGTAACTGCTGCTTTGTCCC	AATCTCCTTCTGGCAGCAGA	Genomic-PCR

Pcgf6	F: ATTTAGGGCACTCTGGGTCC	R1: AACCCTCTCAACATCCTGCA	Genomic-PCR
		R2: CCTCCTCCCCACTCTCTTTC	Genomic-PCR
Ring1a	CCAGCCCTAGTCCTCTCAAC	TAGTCTTCACGTACCTGGGG	Genomic-PCR
Ring1b	F: AGGGCTACACAGAGAAACCG	R1: TACACCCCTCCAGTCTTCAG	Genomic-PCR
		R2: TCACTTGTGAGGGTAGGGG	Genomic-PCR
Pcgf1	CGATGAGGCTTCGGAACCAG	AAAGGAGATGGCTTGCCGAA	RT-PCR
Pcgf2	AAATCACGGAGCTGAACCCT	GGGGAAGTAGGATGGGTAGC	RT-PCR
Pcgf3	ATTGACGCAACCACAGTGAC	CTTGAGAGTGTGGTCCTTGC	RT-PCR
Pcgf4	CGCTTGGCTCGCATTCATTT	GGCAATGTCCATTAGCGTGT	RT-PCR
Pcgf5	ATCTGATCAAGCCCACGACA	CTGTGCAATCTGTCGACGAG	RT-PCR
Pcgf6	GGAGGAGGAAGAGATGAGCC	GTGACAACAGAAGCCAGCTC	RT-PCR
Ring1a	CAGCAAAACGTGGGAACTGA	GCTCTGTGGTTTCCTGCTG	RT-PCR
Ring1b	GCTGGGATGTGGCTATGACA	GCCCAGAGTCATCAGAGGTT	RT-PCR

Table S8. Additional datasets used in this study, related to Figures 2 and 3.

CHIP-Seq		
Name	**Source**	**Identifier**
PCGF1	(Scelfo et al., 2019)	GSE122715
PCGF2	(Scelfo et al., 2019)	GSE122715
PCGF3	(Scelfo et al., 2019)	GSE122715
PCGF5	(Yao et al., 2018)	GSE107377
PCGF6	(Scelfo et al., 2019)	GSE122715
RING1B	(Scelfo et al., 2019)	GSE122715
	(Jaensch et al., 2021)	GSE151899
H2AK119ub1	(Scelfo et al., 2019)	GSE122715
RNA-Seq		
Gene Name	**Source**	**Identifier**
Pcgf2/4-dKO	(Scelfo et al., 2019)	GSE122715

Supplemental Experimental Procedures

Cell culture

ESCs were cultured on gelatinized plates or on mitomycin-treated feeder MEFs in DMEM high glucose (Gibco), which was supplemented with 15% fetal calf serum (Gibco), penicillin-streptomycin (Gibco), 1000U/mL of LIF (Leukaemia inhibitory factor), L-Glutamine (Gibco), non-essential amino acids (Gibco) and β-mercaptoethanol (Sigma).

Colony formation and alkaline phosphatase staining

Resuspended single ESCs were planted on feeder MEFs at an appropriate density for 7-10 days to form colonies, which were washed with PBS twice and fixed with 4% paraformaldehyde (PFA) briefly, and then incubated with staining solution for 15 min at room temperature in dark. Finally, the stained colonies were photographed microscopically.

Teratoma, HE staining and immunohistochemistry

Teratoma formation assay was performed as described(Qin et al., 2021). 10^6 ESCs were trypsinized and resuspended in PBS, which were injected subcutaneously into 8-week-old immunodeficient mice. After 4 weeks, teratomas were fixed with 4% phosphate-buffered formaldehyde at 4°C overnight, and then paraffin-embedded tissue was sliced and stained with hematoxylin and eosin. For immunohistochemistry, paraffin sections were incubated with TROMA-1(markers for endoderm), SMA (markers for mesoderm) and GFAP (markers for ectoderm) respectively and then photographed by BX53 semi-electric fluorescence microscope (Olympus). The experimental animal facility has been accredited by the Association for Assessment and Accreditation of Laboratory Animal Care International, and all the animal work was performed with the approval of the Institutional Animal Care and Use Committee of the Model Animal Research Center of Nanjing University.

Histone extraction and Western blot

Histone extraction was performed as described previously(Qin et al., 2012). Briefly, ESCs were washed with ice-cold PBS, resuspended in Triton extraction buffer (TEB: PBS containing 0.5% Triton X-100 (v/v), 2 mM phenylmethylsulfonyl fluoride (PMSF), 0.02% (w/v) NaN3) and then centrifuged. The nuclear pellet was resuspended in 200 μL 0.2N HCl at 4°C overnight. The supernatants were separated via SDS-PAGE and analyzed by immunoblotting. For whole cell lysates, cells were lysed in RIPA buffer (50 mM Tris pH 8.0, 150 mM NaCl, 5 mM EDTA, and protease inhibitors) on ice, and centrifuged to collect the supernatant for the analysis.

RNA preparation and analysis

RNA was extracted from ESCs with Trizol reagent (Thermo Fisher Scientific) according to the standard protocol. The first strand cDNA was synthesized by HiScript 1st Strand cDNA Synthesis Kit (Vazyme) from total RNA (2.5μg) following the manufacturer's instructions. Gene expression was quantified by RT-qPCR with PowerUp™ SYBR® Green Master Mix (Vazyme) on StepOnePlus™ Real-Time PCR System. The expression of indicated genes was normalized to the content of *β-Actin* mRNA. Primer details are given in table S7 and in a previous report(Qin et al., 2021).

RNA-seq analysis

Total RNA was isolated with Trizol reagent (Invitrogen) from the indicated cell lines according to the manufacturer's instructions, then high-quality RNA sample was quantified with a NanoDrop-1000 spectrophotometer (NanoDrop Technologies) and sequenced by Shanghai Majorbio Bio-pharm Biotechnology Co., Ltd (Shanghai, China). Briefly, RNA-seq transcriptome library was constructed with TruSeq™ RNA sample preparation kit from

Illumina (San Diego, CA), and subsequently, the library was sequenced with Illumina HiSeq 4000. The sequencing data was mapped to mouse genome (Ensemble GRCm38.p5) with orientation mode by TopHat (version2.1.1). For data analysis, the expression of each gene was calculated by FPKM (fragments per kilobase of transcript per million fragments mapped) method. Quantitative analysis of gene abundance and differential expression was performed by RSEM and R statistical package software EdgeR (Empirical analysis of Digital Gene Expression in R). RNA-seq data in this study have been deposited to the Gene Expression Omnibus.

Lentiviral production and infection

Lentiviral supernatants were prepared as described(Qin et al., 2012). Briefly, lentivirus was prepared in HEK293T cells that were cotransfected with the respective lentiviral expression vectors, and a mixture of the packaging plasmids. Virus-containing supernatant was collected at 48h and 72h after transfection, pooled together, passed through a 0.45-μm filter and concentrated by ultra-centrifugation at 4°C. ESCs were infected by the virus particles with Polybrene (Sigma, 8μg/mL). After 24h, the infected cells were selected with puromycin (2 μg/mL) for 1 week and single colonies were picked up and further cultured.

Flow cytometry

ESCs were harvested by trypsin and washed twice with cold PBS. For apoptosis analysis, the cells were stained with fluorescein isothiocyanate-Annexin V (BD Pharmingen) and/or PI for 30 min in dark. For cell cycle analysis, ESCs were fixed with 70% ethanol at -20°C overnight, incubated with RNase A (200g/mL) for 30 min at 37°C subsequently after being washed with PBS, and then stained with PI for 30 min in dark for the analysis by a LSRFortessa flow cytometer equipped with Cell Quest software (BD Biosciences).

Immunofluorescence

ESCs were cultured on gelatin-coated glass coverslips, and then standard immunofluorescence staining protocol was performed. Briefly, ESCs were fixed in 4% (w/v) paraformaldehyde for 15 min at room temperature and rinsed in PBS, and then permeabilised in 0.5% Triton X-100 in PBS for 20 min. After three times washes with PBS, cells were incubated with blocking buffer (PBS, 10% (v/v) goat serum, 1% (w/v) BSA) for 30 min subsequently, to block nonspecific binding sites. After that, ESCs were incubated sequentially with the appropriate dilutions of primary antibody solution at 4°C overnight. Then ESCs were washed with PBS, followed by incubating with fluorophores-conjugated (Alexa Flour 488 or 594 dyes) secondary antibody for 1h in dark. Finally, the cells were counterstained with DAPI (4′,6-diamino-2-phenylindole) in BSA for 5 min for DNA staining. Fluorescent images were taken by Zeiss LSM 880 laser scanning confocal microscope at 63× magnification.

Supplementary References

Huang, Y., Su, T., Wang, C., Dong, L., Liu, S., Zhu, Y., Hao, K., Xia, Y., Jiang, Q., and Qin, J. (2021). Rbbp4 Suppresses Premature Differentiation of Embryonic Stem Cells. Stem cell reports *16*, 566-581.

Huang, Y., Zhao, W., Wang, C., Zhu, Y., Liu, M., Tong, H., Xia, Y., Jiang, Q., and Qin, J. (2018). Combinatorial

Control of Recruitment of a Variant PRC1.6 Complex in Embryonic Stem Cells. Cell reports *22*, 3032-3043.

Jaensch, E.S., Zhu, J., Cochrane, J.C., Marr, S.K., Oei, T.A., Damle, M., McCaslin, E.Z., and Kingston, R.E. (2021). A Polycomb domain found in committed cells impairs differentiation when introduced into PRC1 in pluripotent cells. Molecular cell *81*, 4677-4691.e4678.

Qin, J., Wang, C., Zhu, Y., Su, T., Dong, L., Huang, Y., and Hao, K. (2021). Mga safeguards embryonic stem cells from acquiring extraembryonic endoderm fates. Science advances *7*.

Qin, J., Whyte, W.A., Anderssen, E., Apostolou, E., Chen, H.H., Akbarian, S., Bronson, R.T., Hochedlinger, K., Ramaswamy, S., Young, R.A*., et al.* (2012). The polycomb group protein L3mbtl2 assembles an atypical PRC1-family complex that is essential in pluripotent stem cells and early development. Cell stem cell *11*, 319-332.

Scelfo, A., Fernández-Pérez, D., Tamburri, S., Zanotti, M., Lavarone, E., Soldi, M., Bonaldi, T., Ferrari, K.J., and Pasini, D. (2019). Functional Landscape of PCGF Proteins Reveals Both RING1A/B-Dependent-and RING1A/B-Independent-Specific Activities. Molecular cell *74*, 1037-1052.e1037.

Yao, M., Zhou, X., Zhou, J., Gong, S., Hu, G., Li, J., Huang, K., Lai, P., Shi, G., Hutchins, A.P*., et al.* (2018). PCGF5 is required for neural differentiation of embryonic stem cells. Nature communications *9*, 1463.

Zhao, W., Liu, M., Ji, H., Zhu, Y., Wang, C., Huang, Y., Ma, X., Xing, G., Xia, Y., Jiang, Q*., et al.* (2018). The polycomb group protein Yaf2 regulates the pluripotency of embryonic stem cells in a phosphorylation-dependent manner. The Journal of biological chemistry *293*, 12793-12804.